

## Dielectric properties of BaBi<sub>2</sub>Nb<sub>2</sub>O<sub>9</sub> ceramics

M. Adamczyk · Z. Ujma · M. Pawełczyk

Received: 28 July 2005 / Accepted: 12 October 2005 / Published online: 6 June 2006  
© Springer Science+Business Media, LLC 2006

**Abstract** The crystal structure and dielectric properties as a function of temperature for Ba-based with Bi-layered structure BaBi<sub>2</sub>Nb<sub>2</sub>O<sub>9</sub> (BBN) ceramics were investigated. The obtained results confirmed the relaxor ferroelectric behavior of the studied ceramics, including a strong frequency dispersion of the permittivity maximum and a visible shift of its temperature with frequency. Analysis of the real and imaginary part of permittivity allowed us to determine the values of Burn's temperature and of the freezing temperature characterizing the relaxor ferroelectrics. The physical processes, responsible for the relaxor behavior of the studied ceramics are discussed. The additional low frequency dielectric dispersion at high temperatures in the paraelectric phase range was also observed. Correlation between this dispersion and the thermally stimulated depolarization current was ascertained.

### Introduction

Relaxor ferroelectrics (RF) are a very interesting group of materials, which have been widely described over the last 20 years due to their specific properties. They have found many applications, among others, in multilayer ceramic capacitors, electro-optical devices, ultrasonic and medical imaging devices [1, 2]. Unfortunately majority of them are lead-oxide containing materials and therefore are toxic and

environmentally unfriendly. That is why in recent years new free-lead relaxor ferroelectrics have been explored. Among them Ba-based ferroelectrics with Bi-layered structure—synthesized for the first time by Aurivillius [3]—seems to be a very promising group of materials. The chemical formula of these compounds is (Bi<sub>2</sub>O<sub>2</sub>)<sup>2+</sup>(A<sub>x-1</sub>B<sub>x</sub>O<sub>3x+1</sub>)<sup>2-</sup>, where *x* indicates the number of perovskite building blocks between two (Bi<sub>2</sub>O<sub>2</sub>)<sup>2+</sup> layers and A and B represent the different cations of low and high valences [4]. The layered structure is characterized by a high value of *c*-parameter in comparison with parameters *a* and *b* of the orthorhombic cell and leads up to high anisotropy of the crystallographic structure, which is directly connected with the high anisotropy of electric properties. The best known representative of this family is SrBi<sub>2</sub>Ta<sub>2</sub>O<sub>9</sub>, (SBT), SrBi<sub>2</sub>Nb<sub>2</sub>O<sub>9</sub>, (SBN) and Ba<sub>1-x</sub>Sr<sub>x</sub>Bi<sub>2</sub>Nb<sub>2</sub>O<sub>9</sub>, (BSBN). Recently, the interest in Bi-layered perovskites has increased due to their excellent stability against repetitive switching (fatigue endurance) [5], fast switching speed and good piezoelectric properties [6]. Therefore, these materials are now intensively investigated in view of their potential applications in electronics. Particularly SBT is considered to be a promising material for ferroelectric non-volatile semiconductor memory (FeRAMs) and optoelectronic-integrated devices [5, 7].

Investigations of the other representative of the Aurivillius family, BaBi<sub>2</sub>Nb<sub>2</sub>O<sub>9</sub>, (BBN), the compound, which seems to be very interesting from the point of view of the relaxor behavior, are presented in this paper. BBN, less studied so far, is a relaxor material of a tetragonal structure with a I4/mmm space group [8]. The aim of our paper is to present experimental results of the dielectric properties of BBN ceramics in comparison with lead containing relaxor ferroelectrics such PLZT and PBZT, reported in our earlier papers [9–11].

M. Adamczyk (✉) · Z. Ujma · M. Pawełczyk  
Institute of Physics, University of Silesia, ul. Uniwersytecka 4,  
40-007 Katowice, Poland  
e-mail: madamczy@us.edu.pl

## Ceramics preparation

The  $\text{BaBi}_2\text{Nb}_2\text{O}_9$  ceramics were prepared using the conventional mixed-oxide processing technique. Stoichiometric amounts of  $\text{BaCO}_3$ ,  $\text{Bi}_2\text{O}_3$ ,  $\text{Nb}_2\text{O}_5$  reagents were weighed and mixed. Thermal synthesis of the pressed mixture was carried out at  $950^\circ\text{C}$  for 2 h. Then the crushed, milled and sieved materials were pressed again into cylindrical pellets and sintered at  $1100^\circ\text{C}$  for 6 h and then cooled to room temperature for 12 h. The obtained ceramics were semitransparent and of good mechanical quality. The Archimedes displacement method with distilled water was employed to evaluate the sample density. The bulk density of BBN ceramics was equal to  $7.07\text{ g/cm}^3$ . The obtained ceramic cylinders were cut into 0.6 mm layers, polished and coated with silver paste electrodes without thermal treatment.

## Results and discussion

The grain structure and distribution of all elements throughout the grains was examined by scanning electron microscope, (SEM), JSM-5410 with an energy dispersion X-ray spectrometer (EDS). The grain size measurements were performed on the fractured surface of ceramics. The samples were broken at ambient atmosphere, then covered with sputtered gold and placed in a vacuum ( $10^{-5}$  Torr) chamber of the electron microscope. A typical scanning electron image of the BBN ceramics is shown in Fig. 1. The average grain size was ca.  $2\ \mu\text{m}$ . Energy dispersion X-ray spectrometer was used to check the distribution of individual elements within the grains. The microanalysis was performed with ISIS-300 SEMQuant programme. The EDS analysis indicated a fairly homogenous distribution of all elements (Ba, Bi, Nb and O) throughout the grains.

The X-ray diffraction pattern (XRD) of BBN ceramics obtained at room temperature is shown in Fig. 2. XRD measurements were carried out on powdered samples using a high resolution Siemens diffractometer ( $\theta$ - $\theta$ ) D 5000 with filtered  $\text{Cu K}\alpha$  radiation (40 kV, 30 mA). The powder diffraction diagram was measured from  $10$  to  $100^\circ$  in  $2\theta$  with  $0.02^\circ$  steps and a 2 s counting time. The XRD profile was analyzed by using a set of programs i.e. DHN Powder Diffraction System ver.2.3. The location and intensity of 32 diffraction lines were identified in the range of the measured angle. The obtained results show a good agreement with JCPDS standard number 12-0403 for  $\text{BaBi}_2\text{Nb}_2\text{O}_9$ . All line indexes connected with the Aurivillius structure were assigned. The appearance of a single very weak line for  $2\theta = 25.58^\circ$  not connected with the Aurivillius structure is in our opinion caused by the presence of a small quantity of  $\text{BaCO}_3$  since this line corresponds the strongest

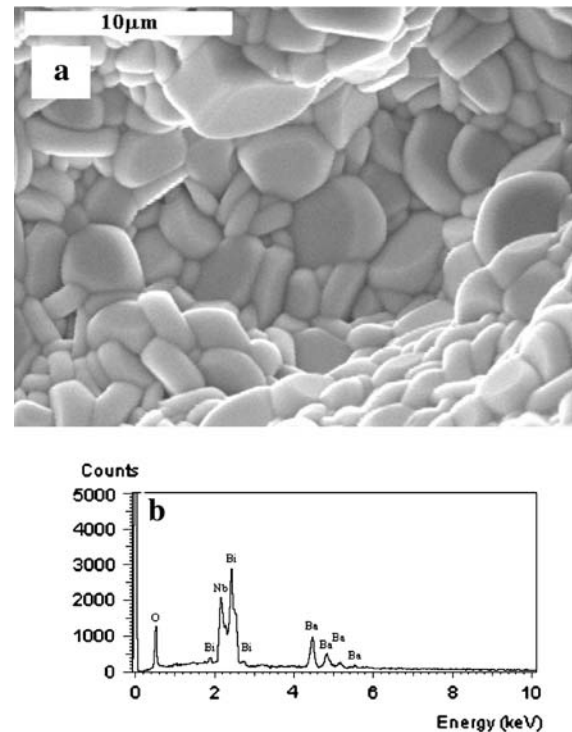


**Fig. 1** SEM images of the fractured surface (a) and the EDS analysis (b) of BBN ceramics

diffraction line of  $\text{BaCO}_3$  structure (JCPDS standard No. 11-0697). The ratio of the integral intensity of this line to the integral intensity of all the lines of the diffraction pattern allowed us to estimate the content of the  $\text{BaCO}_3$  phase at ca. 0.5%. The lattice parameters obtained from X-ray pattern were  $a = b = 3.9406 \pm 0.0006\ \text{\AA}$ , and  $c = 25.6378 \pm 0.0059\ \text{\AA}$ . These results are in a good agreement with the results reported in [12].

The dielectric measurements of real ( $\epsilon'$ ) and imaginary ( $\epsilon''$ ) parts of permittivity versus temperature were carried

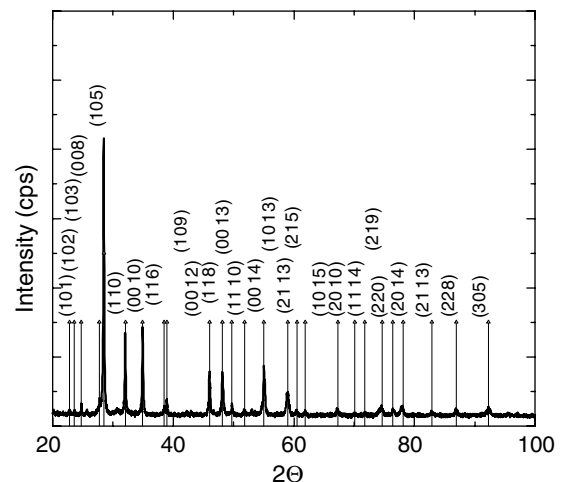


**Fig. 2** XRD pattern of BBN ceramics

out on heating by using impedance analyzer HP4192A. The sample was deaged by thermal treatment at 723 K prior to measurements to allow recombination and relaxation of part of the frozen defects, formed during the sintering process. The characteristics  $\epsilon'(T)$  and  $\epsilon''(T)$  for a number of frequencies are shown in Fig. 3. These characteristics, and in particular  $\epsilon'(T)$  curves, reveal a strongly diffused phase transition which is caused by Ba ions entering not only the perovskite blocks but also  $(\text{Bi}_2\text{O}_2)^{2+}$  layers resulting in inhomogeneous distribution of Ba ions and local charge

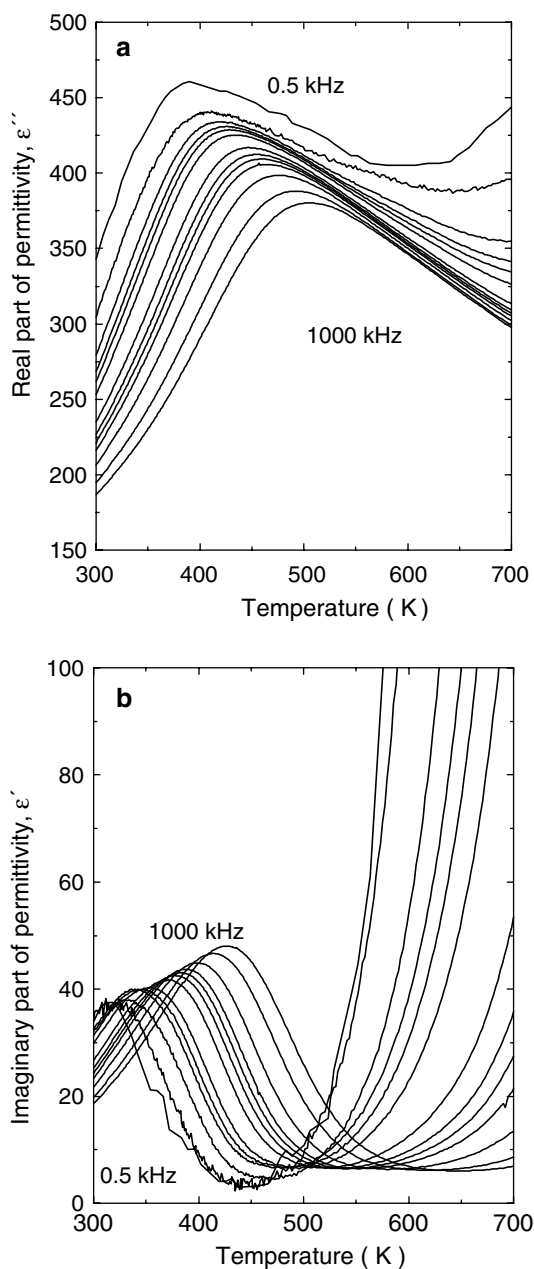


**Fig. 3** Real (a) and imaginary (b) parts of permittivity as a function of temperature measured at various frequencies of the measuring field. The individual curves concern the following frequencies: 0.5; 1; 3; 5; 7; 10; 30; 50; 70; 100; 200; 500 and 1000 kHz

imbalance in the layered structure [13]. In this way Ba-induced disorder in the layered structure leads to the broadening of the dielectric response and to the intensification relaxor properties of these ceramics [14]. Ismunadar et al. [12] showed, on the basis of XRD measurements that in BBN ceramics 15–20% of  $\text{Ba}^{2+}$  ions are located in the  $(\text{Bi}_2\text{O}_2)^{2+}$  layers. The frequency dependence of the dielectric response demonstrates the behavior typical for relaxor ferroelectrics i.e. the significant reduction of  $\epsilon'_{\text{max}}$  and shift of the corresponding temperature ( $T_m$ ) towards higher values with frequency increase. This behavior is similar to lead containing relaxor ferroelectrics such as PMN, PLZT [15, 16] and PBZT [10] ceramics, except for much lower value of the real part of permittivity. Such a great difference in the value of  $\epsilon'_{\text{max}}$  may be the consequence of a much lower polarizability of  $\text{Ba}^{2+}$  ions in comparison with  $\text{Pb}^{2+}$  ions. The weak interaction between dipole moments in the layered structure (in comparison with cubic perovskite structure of lead containing relaxors) should be also taken into consideration [17]. On the other hand it should be stressed that in the present case the  $T_m$  shift with frequency is much stronger than for PMN or PBZT 25/70/30 ceramics. In the case of BBN ceramics  $\Delta T_m$  (defined as the difference between the  $T_m$  measured at 0.1 kHz and that measured at 20 kHz) is equal to ca. 92.6 K, whereas for PBZT 25/70/30 ceramics  $\Delta T_m=7.3$  K [10].

The frequency dependencies of dielectric response for several selected temperatures are shown in Fig. 4. As can be seen the real part of permittivity gradually decreases with increasing frequency. The character of  $\epsilon''(f)$  changes is more complicated. At low temperatures the broadened maximum in the  $\epsilon''(f)$  curve occurs and the greatest values of  $\epsilon''$  are observed for low frequency. The maximum gradually increases and shifts to high temperatures. The broad Cole–Cole ‘‘circular-arc’’, shown in Fig. 5, indicates a broad distribution of relaxation times [18] which suggests that the concept of the Vogel–Fulcher relationship has to be used to describe the shift of the real part of the permittivity peak with frequency instead of the classic Debye relaxation [19]:

$$f = f_0 \exp \left[ \frac{-E_a}{k(T_m - T_f)} \right] \tag{1}$$

where  $E_a$  is the activation energy,  $T_f$  is the freezing temperature of polarization fluctuation, and  $f_0$  is the pre-exponential factor. The plot relating frequency to the  $T_m$  fitted to the Vogel–Fulcher relationship is shown in Fig. 6. The values of the fitting parameters, especially the freezing temperature, are significantly different from those observed for lead containing relaxor ferroelectrics such as PMN or PLZT. For example for PMN and PLZT ceramics the parameters  $E_a$ ,  $T_f$  and  $f_0$  equal 0.08 eV, 217 K,  $10^{12}$  Hz and

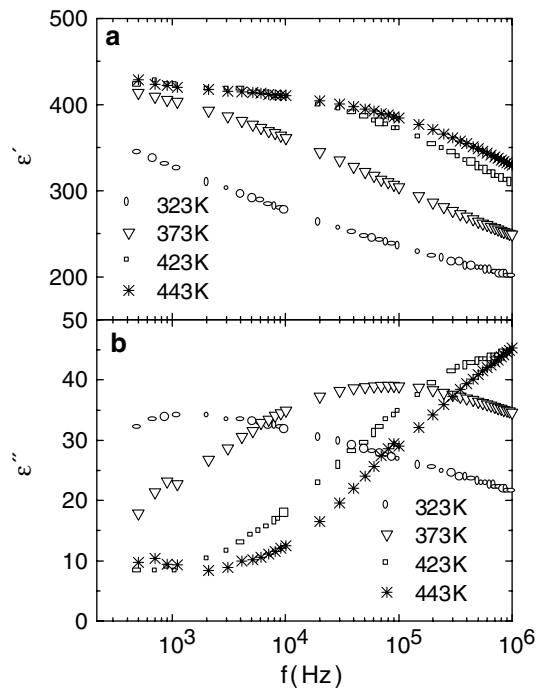


**Fig. 4** Frequency dependences of the complex components of permittivity for given temperatures

0.12 eV, 249 K,  $6 \cdot 10^{13}$  Hz, respectively [15, 16]. It should be noticed that the value of  $T_f$  obtained for BBN ceramics by Kholkin et al. [6] and us are also different (170 and 97 K, respectively). In our opinion, it may be caused by different technological conditions during ceramic preparation. The various sintering conditions (sintering temperature and time) result in the change in structural disorder and influence the value and dynamics of the dipole moments. The dynamics of the dipoles, associated with the thermally activated flips, is considered to be responsible for the properties of RF.

The chemical disorder mentioned above caused by  $\text{Ba}^{2+}$  ions is probably also responsible for the relaxor behavior of the BBN ceramics. It is commonly known that the dielectric properties of RF are explained in literature in terms of small regions of local polarization (so called polar-regions), which appear at temperatures much higher than  $T_m$  (at the

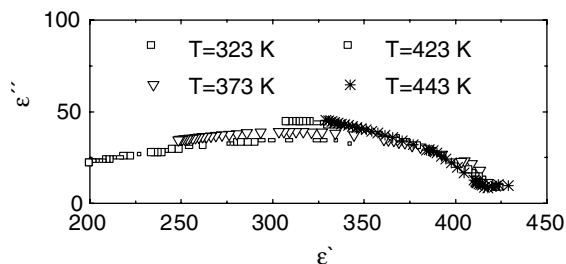


**Fig. 5** Cole–Cole plots for BBN ceramics at various temperatures

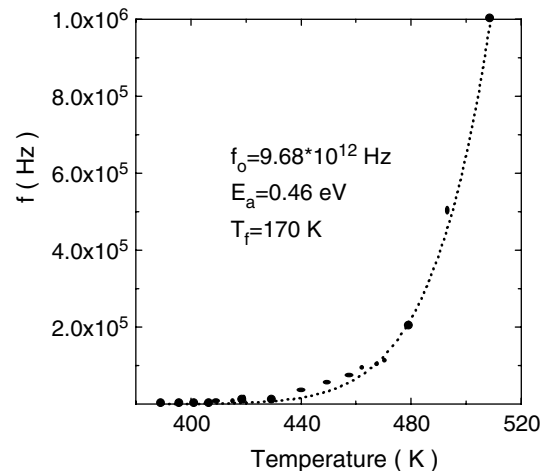


**Fig. 6** Measurement frequency as a function of temperature  $T_m$ . Points are experimental; the dot line is the fitting of the Vogel–Fulcher relationship

Burn's temperature,  $T_B$ ) [20–22]. Therefore, the  $\varepsilon'(T)$  deviates from the Curie–Weiss law below  $T_B$  and obeys this law above  $T_B$ . The temperature dependence of a local order parameter  $q(T)$  was calculated from the Curie–Weiss formula modified by Sherrington and Kirkpatrick [23, 24]:

$$\varepsilon' = \frac{C\{1 - q(T)\}}{T - \theta\{1 - q(T)\}} \quad (2)$$

where  $\theta$  is the Curie–Weiss temperature,  $C$  is the Curie–Weiss constant and are equal to 314.12 K and  $1.9 \cdot 10^5$  K, respectively. The temperature dependence of the local order parameter obtained from 100 kHz dielectric response is shown in Fig. 7. The value of  $q$  is equal to zero at high temperatures in the paraelectric phase and starts to increase as soon as the polar clusters begin to appear on cooling, i.e. at  $T_B$ . The  $T_B$  calculated from Eq. (2) is equal to 672 K. It is worth noticing that the  $q(T)$  is frequency dependent however the dependence of temperature  $T_B$  on frequency is very weak [24].

The dielectric properties of Ba-based layered perovskites are different from those of the lead containing RF governed by the dynamics of polarization clusters. The small  $\text{Bi}^{3+}$  ions ( $R = 0.96 \text{ \AA}$ ) substituted for Ba in oxygen octahedra blocks can be easily shifted even further from the central A-positions of the perovskite cell, than the large  $\text{Ba}^{2+}$  ions ( $R = 1.34 \text{ \AA}$ ). However, due to high anisotropy and a large value of the  $c$ -parameter, confirmed by X-ray measurements [6], the distance between clusters is significantly bigger than in the classical relaxors and hence the interaction between them is more difficult. Probably this is why the formation of the normal ferroelectric state is only possible at low temperatures. Moreover, the freezing temperature is much lower than for Pb-containing RF. The

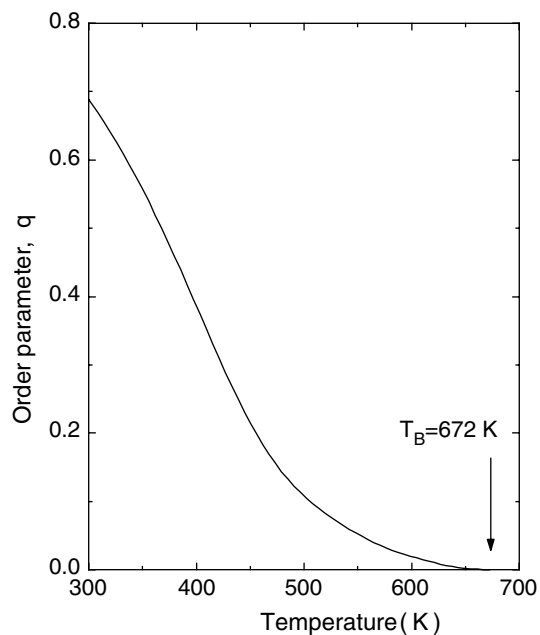


**Fig. 7** Temperature dependence of the local order parameter calculated from data  $\epsilon'(T)$  measured at frequency 100 kHz

weak interactions between dipole moments in layered structure in connection with small polarizability of  $\text{Ba}^{2+}$  ions (in comparison with  $\text{Pb}^{2+}$  ions) may be the reason for the small value of permittivity [25]. The low value of  $T_f$  makes it impossible to observe ferroelectric hysteresis loops below the temperature of dielectric maximum in Ba-based Bi-layered perovskites [14].

In Fig. 3 it can be seen that the studied BBN ceramics demonstrate low frequency dispersion at high temperatures of the paraelectric phase. This additional dispersion is often found in ferroelectric ceramics of perovskite structure [26–27] and originates from the non-homogeneous distribution of ion space charges participating in the screening process of the polar-regions [9]. The occurrence of the polar-regions and their interaction with free electron and ion space charges can be identified by thermally stimulated depolarization current (TSDC) studies [9, 10, 28]. The samples were first polarized at dc field with strength  $E_p$ , applied for 10 min at various temperatures ( $T_p$ ) and then cooled in the field to 273 K at which the field was switched off. The samples were then heated with a constant rate of 5 K/min to the temperature of 723 K. The temperature changes of the observed TSDC are shown in Fig. 8. The TSDC with broadened maximum appeared at temperatures higher than the temperature at which the ceramics were pre-polarized. The shift of this maximum results from a mutual interaction of the orientation (dipole) part of the metastable polarization and the polarization of the free ion and electron space charges, participating in the screening process of the polar-regions [28]. The evident correlation

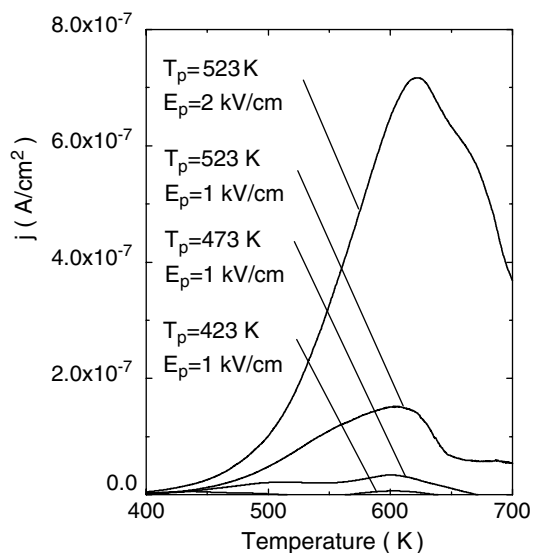


**Fig. 8** Thermally stimulated depolarization currents versus temperature for BBN ceramics

between the temperature changes of the TSDC on one hand and the low frequency dispersion in the paraelectric phase on the other hand can be noticed. We reported the problem of similar correlation in lead containing RF such as PLZT and PBZT ceramics and gave a more detailed interpretation in our previous papers [9–11, 29].

## Conclusions

1. The investigated ceramics show a behavior typical for relaxor ferroelectrics but the temperature range of their occurrence is significantly wider than for lead containing relaxors such as PMN, PLZT or PBZT.
2. Two different types of dielectric relaxation are observed for BBN ceramics. The first appears in the vicinity of the temperature corresponding to the maximum in real part of permittivity and obeys the Vogel–Fulcher relationship with the freezing temperature much lower than the permittivity maximum ( $T_f = 170$  K). The second type of dielectric dispersion for low frequencies occurs at a high temperature range in the PE phase.
3. Correlation between low frequency dispersion and the thermally stimulated depolarization current was proved.

## References

1. Galassi C, Piazza D, Craciun F, Verardi P (2004) *J Europ Ceram Soc* 24:1525
2. Cross LE (1994) *Ferroelectrics* 151:305

3. Aurivillius B (1949) *Ark Kemi* 1:463
4. Scott JF, Ross FM, Paz de Araujo CA, Scott MC, Huffman M (1996) *MRS Bul* 21:33
5. Paz de Araujo CA, Cuchiaro JD, McMillan LD, Scott MC, Scott JF (1995) *Nature (London)* 374:627
6. Kholkin AL, Brooks KG, Setter N (1997) *Appl Phys Lett* 71:2044
7. Scott JF (1998) *Ferroelectrics Rev* 1:1
8. Shimakawa Y, Kubo Y, Nakagawa Y, Goto S, Kamiyama T, Asano H, Izumi F (2000) *Phys Rev B* 61:6559
9. Hańderek J, Ujma Z, Carabatos-Nedelec C, Kugel GE, Dmytrów D, El-Harrad I (1993) *J Appl Phys* 73:367
10. Ujma Z, Adamczyk M, Hańderek J (1998) *J Europ Ceram Soc* 18:2201
11. Adamczyk M, Ujma Z, Hańderek J (2001) *J Appl Phys* 89:542
12. Ismunadar, Kennedy BJ (1999) *J Mater Chem* 9:541
13. Smolensky GA, Izupov VA, Agranovkaya AI (1961) *Sov Phys Solid State* 3:651
14. Kholkin AL, Avdeev M, Costa MEV, Baptista JL, Dorogotsev SN (2001) *Appl Phys Lett* 79:662
15. Viehland D, Wuttig M, Cross LE (1991) *Ferroelectrics* 120:71
16. Shur V, Kuminov V, Lomakin G, Beloglazov S, Slovikovski S, Krumins A, Sternberg A (1998) *J Korean Phys Soc* 32:S985
17. de Costa GC, Simoes AZ, Ries A, Foschini CR, Zaghetta MA, Varela JA (2004) *Matt Lett* 58:1709
18. Fan HQ, Zhang LT, Zhang LY, Yao X (1999) *Solid State Commun* 111:541
19. Viehland D, Jang S, Cross LE, Wuttig M (1990) *J Appl Phys* 68:2916
20. Cross LE (1987) *Ferroelectrics* 76:241
21. Cheng Z-Y, Katiyar RS, Yao X, Bhalla AS (1998) *Phys Rev B* 57:8166
22. Bovtun V, Petzelt J, Porokhonskyy V, Kamba S, Yakimenko Y (2001) *J Europ Ceram Soc* 21:1307
23. Sherrington D, Kirkpartick S (1975) *Phys Rev Lett* 35:1792
24. Viehland D, Jang SJ, Cross LE, Wuttig M (1992) *Phys Rev B* 46:8003
25. Miranda C, Costa MEV, Avdeev M, Kholkin AL, Baptista JL (2001) *J Europ Ceram Soc* 21:1303
26. Bidault O, Goux P, Kchikech M, Belkaoumi M, Maglione M (1994) *Phys Rev B* 49:7868
27. Maglione M (1996) *Ferroelectrics* 176:1
28. Braunlich P (1979) *Thermally stimulated relaxation in solids, topics in applied physics, vol. 37*, Springer, Berlin
29. Hańderek J, Adamczyk M, Ujma Z (1999) *Ferroelectrics* 233:253